Crystal structure transformations in SiO_2 from classical and *ab initio* metadynamics

ROMAN MARTOŇÁK[1]*, DAVIDE DONADIO[1], ARTEM R. OGANOV[2] AND MICHELE PARRINELLO[1]

[1]Computational Science, Department of Chemistry and Applied Biosciences, ETH Zurich, USI Campus, Via Giuseppe Buffi 13, CH-6900 Lugano, Switzerland
[2]Laboratory of Crystallography, Department of Materials, ETH Zurich, HCI G 515, Wolfgang-Pauli-Str. 10, CH-8093 Zurich, Switzerland
*e-mail: martonak@phys.chem.ethz.ch

Published online: 16 July 2006; doi:10.1038/nmat1696

Silica is the main component of the Earth's crust and is also of great relevance in many branches of materials science and technology. Its phase diagram is rather intricate and exhibits many different crystalline phases[1–6]. The reported propensity to amorphization and the strong influence on the outcome of the initial structure and of the pressurization protocol[1,7] indicate the presence of metastability and large kinetic barriers. As a consequence, theory is also faced with great difficulties and our understanding of the complex transformation mechanisms is still very sketchy despite a large number of simulations[8–13]. Here, we introduce a substantial improvement of the metadynamics method[14,15], which finally brings simulations in close agreement with experiments. We unveil the subtle and non-intuitive stepwise mechanism of the pressure-induced transformation of fourfold-coordinated α-quartz into sixfold-coordinated stishovite at room temperature. We also predict that on compression fourfold-coordinated coesite will transform into the post-stishovite α-PbO_2-type phase. The new method is far more efficient than previous methods, and for the first time the study of complex structural phase transitions with many intermediates is within the reach of molecular dynamics simulations. This insight will help in designing new experimental protocols capable of steering the system towards the desired transition.

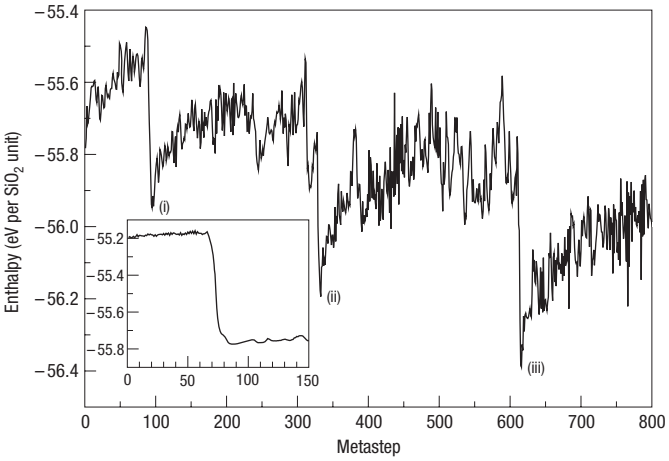

Figure 1 Evolution of the enthalpy in the simulation starting from quartz II. Inset: enthalpy during the simulation starting from α-quartz. The simulation was carried out at $T = 300$ K and $p = 150$ kbar.

A challenge in the experimental and theoretical study of SiO_2 is its propensity to amorphize on compression[7]. At room temperature only the application of slow compression allowed phase transformations to be observed experimentally. Starting from α-quartz and using different experimental protocols, transitions to poorly crystallized stishovite above 600 kbar (ref. 2), to metastable quartz II at 220 kbar (ref. 3), and more recently to a monoclinic $P2_1/c$ phase at 450 kbar (ref. 5) have been reported. Polymorphism in silica has been studied theoretically by total energy calculations[16–18], where the energetics of possible polymorphs are confronted, or by molecular dynamics (MD) simulations using the Parrinello–Rahman method[19], with empirical force fields[8–11,13] and with on-the-flight *ab initio* computed interactions[12]. However, static calculations have to rely on educated guesses on the possible structures and offer no clue as to the dynamics. On the other hand, the great metastability and the tendency of SiO_2 to amorphize have severely hampered dynamical studies. Recently, we proposed a new approach[14] based on the ideas of metadynamics[15]. The new scheme has successfully been applied to a variety of inorganic and organic systems[20–23]. As this approach has demonstrated a considerably improved ability to find new crystal structures, we have applied it to several silica phases at various pressures. However, when confronted with a complex case, such as SiO_2, even this powerful method failed to reproduce many of the experimentally observed structures. In particular, the structural transitions often resulted in an amorphous structure. This prompted us to improve on the scheme of ref. 14, bringing the simulation into agreement with the experiments and allowing novel predictions to be made.

Metadynamics is a scheme for exploring the free-energy dependence on a few carefully selected collective coordinates. Inspired by the work of Parrinello and Rahman[19], we use

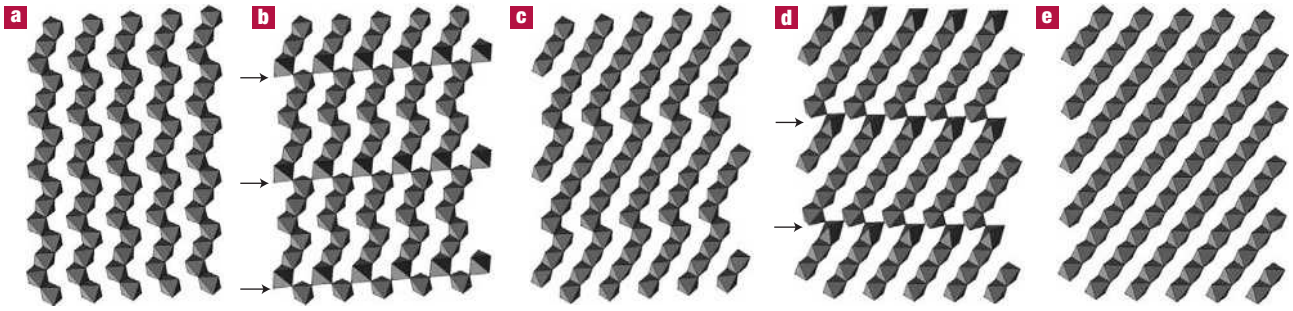

Figure 2 Transition from the 3 × 2 structure to stishovite. a–e, Two steps of the transition from the 3 × 2 structure (**a**) to stishovite (**e**). Elimination of the kinking of octahedral chains proceeds via an intermediate 6 × 2 structure (**c**). The arrows denote the presence of corner-sharing octahedra in the transition states (**b**) and (**d**).

the simulation box edges $\mathbf{h} = (\mathbf{a}, \mathbf{b}, \mathbf{c})$ as collective coordinates for exploring structural phase transitions in crystals. Although highly successful, this choice does not take into account that the Gibbs free energy, which is the relevant thermodynamic potential at temperature T and pressure P, is a highly anisotropic function of $\mathbf{h}$. In particular, a crystal is much more resistant to deformations that change the volume than to other types of strain. To treat all types of deformation the same, we introduced new scaled collective coordinates. We freeze the box rotations by assuming the matrix $\mathbf{h}$ to be upper triangular[20] and write the six-dimensional order parameter as $\tilde{\mathbf{h}} = (h_{11}, h_{22}, h_{33}, h_{12}, h_{13}, h_{23})^{\mathrm{T}}$. Close to a given equilibrium crystal structure characterized by a matrix $\tilde{\mathbf{h}}^0$, the Gibbs free energy can be written as $\mathcal{G}(\tilde{\mathbf{h}}) \approx \mathcal{G}(\tilde{\mathbf{h}}^0) + (1/2)(\tilde{\mathbf{h}} - \tilde{\mathbf{h}}^0)^{\mathrm{T}}\mathbf{A}(\tilde{\mathbf{h}} - \tilde{\mathbf{h}}^0)$, where the hessian matrix $A_{ij} = \partial^2\mathcal{G}(\tilde{\mathbf{h}})/\partial\tilde{h}_i\partial\tilde{h}_j|_{\tilde{\mathbf{h}}_0}$ can be calculated from finite differences of pressure tensor or from the $\mathbf{h}$ matrix fluctuations in a constant-pressure simulation. At equilibrium, the $\mathbf{A}$ matrix has positive real eigenvalues $\{\lambda^i\}$ and can be diagonalized by an orthogonal matrix $\mathbf{O}$. The largest of the eigenvalues $\{\lambda^i\}$ is usually associated with the volume change and is typically more than an order of magnitude larger than the smallest one; therefore, the initial well has the shape of a long and narrow valley. To eliminate sampling problems resulting from such a highly anisotropic shape, we choose as new collective coordinates the variables $s_i = \sqrt{\lambda^i}\sum_j O_{ji}(\tilde{h}_j - \tilde{h}^0_j)$. With this choice the well becomes spherical $\mathcal{G}(\mathbf{s}) \approx \mathcal{G}(\tilde{\mathbf{h}}^0) + (1/2)\sum_i s_i^2$. The thermodynamic force $\partial\mathcal{G}/\partial s_i$ reads

$$\frac{\partial\mathcal{G}}{\partial s_i} = \sum_j \frac{\partial\mathcal{G}}{\partial\tilde{h}_j} O_{ji} \frac{1}{\sqrt{\lambda^i}},$$

where $-\partial\mathcal{G}/\partial h_{ij} = V[\mathbf{h}^{-1}(\mathbf{p} - P)]_{ji}$ (refs 14,20), $\mathbf{p}$ is the averaged microscopic pressure tensor and $V = \det\mathbf{h}$ is the volume of the system. In terms of these variables, the metadynamics equations[14,15] become

$$\mathbf{s}^{t+1} = \mathbf{s}^{\mathrm{t}} + \delta s \frac{\phi^{\mathrm{t}}}{|\phi^{\mathrm{t}}|},$$

$$\mathcal{G}^{\mathrm{t}}(\mathbf{s}) = \mathcal{G}(\mathbf{s}) + \sum_{t'<t} W \mathrm{e}^{-|\mathbf{s}-\mathbf{s}^{t'}|^2/2\delta s^2}$$

and $\phi^{\mathrm{t}} = -\partial\mathcal{G}^{\mathrm{t}}/\partial\mathbf{s}$. The history-dependent term in $\mathcal{G}^{\mathrm{t}}(\mathbf{s})$ pushes the system out of the local minimum. The width δs of the gaussian is chosen such that its effect is substantially larger than the thermal fluctuation, that is, $\delta s \gg \sqrt{k_{\mathrm{B}}T}$. Here we shall use the prescription of ref. 14, which relates the gaussian height W to the gaussian width δs, in the form $W \sim \delta s^2$. Ideally after a phase transition one should stop, recalculate the hessian and redefine the coordinates s_i. Actually, in most cases this is not necessary and the same set of coordinates can be used to study a whole sequence of transitions. However, occasionally, the change in the hessian might be so large that a redefinition of s_i is necessary.

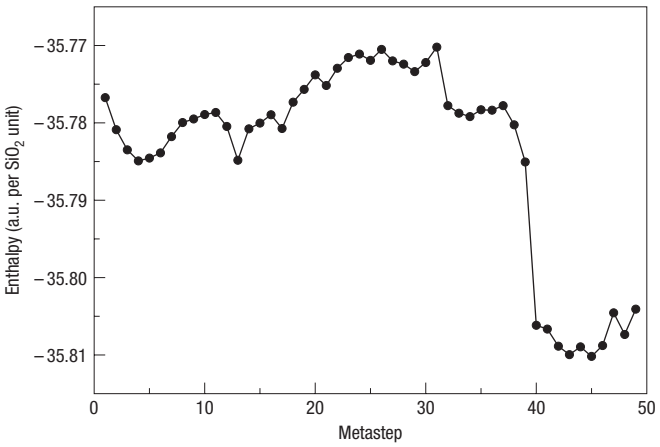

Figure 3 Evolution of the enthalpy during the transition from coesite to the α-PbO_2 phase. The *ab initio* simulation was carried out at $T = 600$ K and $p = 220$ kbar.

Most of our extensive simulations were conducted using the force field by van Beest, Kramer and van Santen (BKS)[24], which has recently been shown to qualitatively reproduce the phase boundaries between quartz, coesite and stishovite[25]. We work at room temperature, where the free-energy barriers for transitions are expected to be high. We first applied metadynamics to a 324-atom supercell of α-quartz at $p = 150$ kbar where α-quartz is still mechanically stable, using $\delta s = 30$ (kbar Å^3)$^{1/2}$ and $W = 900$ kbar Å^3. Figure 1 shows the time evolution of the enthalpy during a metadynamics run. At $T = 300$ K, the enthalpy of silica is very close to its Gibbs free energy. The inset in the figure shows the first transformation from α-quartz to quartz II, which has also been reported by other authors[9,10,13,26]. It takes place after 88 metasteps and is almost barrier-less. In quartz II (space group $C2$), the Si atoms are arranged in alternating layers of tetrahedral and octahedral coordination. Because we observed a big change in the elastic properties, we decided to change collective coordinates and use in the continuation of

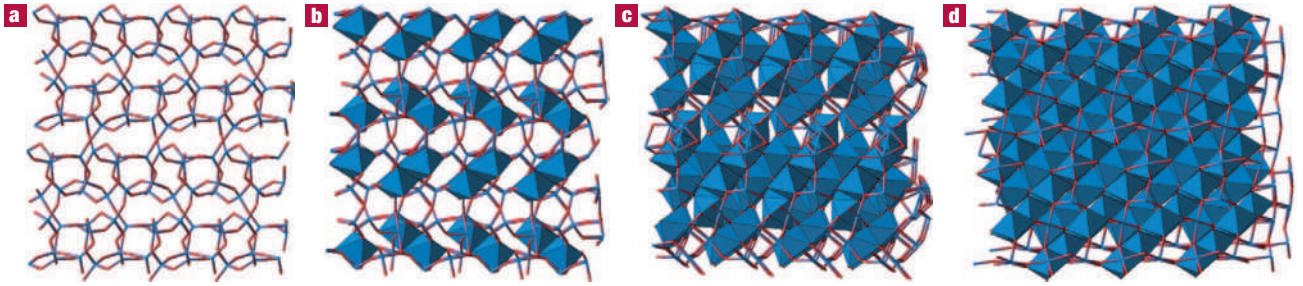

Figure 4 Transition from coesite to the α-PbO_2 phase. a–d, Structural evolution during the transition from coesite (**a**) to the α-PbO_2 phase (**d**). Intermediate states (**b**) and (**c**) show the initial growth and competition of chains of octahedra in different planes.

the run $\{\lambda_i\}$ and **O** appropriate for quartz II, with parameters $\delta s = 100$ (kbar Å^3)$^{1/2}$ and $W = 20{,}000$ kbar Å^3. Figure 1 shows the behaviour of the enthalpy after the transition to quartz II. Three different abrupt transitions, which occur after rather high barriers are overcome, can easily be identified. In the first transition (i) fourfold-coordinated silicon atoms disappear and a distorted octahedral structure with bond lengths of up to 2.4 Å is created. The octahedra are arranged in planes where they form kinked edge-sharing chains with a 3×2 periodicity. The 3×2 pattern represents a particular case of a family of structures discussed in ref. 17, where it was shown that low-enthalpy octahedral structures of silica are characterized by chains of edge-sharing octahedra with various degrees of kinking and ABAB stacking. In the structure (i), however, the stacking of the close-packed planes is not ABAB but instead is ABC. This structure is an intermediate step before the transition to a lower enthalpy structure (ii) (Fig. 1). By decompressing the latter structure to $p = 0$ and calculating its diffraction pattern we found that it is identical to that corresponding to the 3×2 $P2_1/c$ structure found experimentally in the recovered sample in ref. 5. Such a phase has ABAB stacking and belongs to the family of structures discussed in ref. 17. The transition (iii) starting at metastep 610 finally leads, at metastep 616, to stishovite, which is the equilibrium structure at this pressure[25]. It is interesting to examine how this transition takes place. In the 3×2 $P2_1/c$ structure, the kink repeats itself every three octahedra (Fig. 2a), whereas stishovite is characterized by straight chains of octahedra (Fig. 2e). The transition therefore requires that the kinks are eliminated. The path followed by the system is shown in Fig. 2, where two steps can clearly be identified. During metastep 612 (Fig. 2a–c), the system eliminates half of the kinks and the structure (2c) corresponds to a 6×2 pattern. The transformation is based on a concerted bond-switch mechanism that occurs at the kinks and proceeds via a transition state (2b) where the octahedra involved in the transition temporarily share their corners. In the second part of the transition, which takes place at metastep 614 (Fig. 2d,e), the remaining kinks are eliminated and the chains become straight (2e). This transition also involves temporary formation of corner-sharing octahedra (2d). The evolution of the supercell during the transitions at metasteps 610–616 can be viewed as a shearing mode in the (010) plane of stishovite and only a tiny change in volume takes place. An intuitive crystallographic pathway for such reconstructive transitions would correspond to a maximum common subgroup of the symmetry groups of the starting and final structures, usually involving small supercells[27]. For transitions between close-packed silica structures, such intuition would produce a mechanism based on nearly fixed oxygen atoms and the silicon atoms migrating into the empty octahedral voids. The transition mechanism we observe is very different: it occurs in two stages and involves large supercells and crystallographic shear of large portions of the structure. Metadynamics proposed a similar mechanism for the post-perovskite transition in $MgSiO_3$ (ref. 22). This work is the first case where MD simulations have been able to go beyond quartz II.

We have repeated these calculations with a variety of cell sizes and slightly different pressures, and also using different metadynamics parameters. As in real-life experiments, the outcome is dependent on the protocol used. In some cases the simulation leads to an amorphous structure, in others to defective phases with kinked chains or to a transition from α-quartz to quartz II followed by a direct transition to stishovite. The most surprising finding was a transition to an anatase structure ($I4_1/amd$), which so far has not been reported for silica. A static density-functional theory calculation using a generalized gradient approximation (GGA) exchange–correlation functional showed that the anatase structure, although it has the lowest energy in a narrow range of volumes, is not the lowest-enthalpy phase at any pressure (structural parameters of the anatase, $P2_1/c$ and $C2$ structures optimized by *ab initio* calculations are included in Supplementary Information). In contrast, the same calculation carried out with the BKS potential shows a phase boundary between coesite and anatase at −26 kbar and another one between anatase and stishovite at 102 kbar. Therefore, the anatase phase represents a so far unknown artefact of the BKS potential. This finding demonstrates the excellent ability of our approach to find hitherto unexpected structures, and suggests that this feature can also be used as a stringent test of model potentials.

In a run at $p = 0$ starting from an α-quartz sample consisting of 144 atoms with $\delta s = 50$ (kbar Å^3)$^{1/2}$ and $W = 4{,}000$ kbar Å^3, we ended up with a tetrahedrally coordinated structure with space group $Ibam$ containing besides six- and eight-membered rings also four-membered rings. This is a structure also known as orthorhombic moganite[28], which is very close to monoclinic moganite found in nature. This simulation was also part of a quest to find a transition to coesite, which is already stable at $p < 0$ within the BKS potential[25]. Just like the experimentalists working at room temperature, we failed. However, because studying the behaviour of this phase is of great interest, we decided to start directly from coesite, for which at room temperature only pressure-induced amorphization has been reported[7].

Coesite is a complex tetrahedral structure with a conventional unit cell containing 48 atoms. We used such a single unit cell in the simulation and used our metadynamics method together with the *ab initio* Car–Parrinello scheme[29] at 220 kbar and 600 K. We used parameters $\delta s = 40$ (kbar Å^3)$^{1/2}$ and $W = 1{,}600$ kbar Å^3. In 40 metasteps we found a direct transition from coesite to the metastable α-PbO_2 structure. The evolution of enthalpy

and structure is shown in Figs 3 and 4. The initial tetrahedral network topology of coesite (Fig. 4a) starts to change after the first 10 metasteps. Threefold-coordinated oxygens are formed and the large rings from 9 to 12 members, which are characteristic for coesite, transform into smaller ones. The arrays of octahedra formed at this initial stage lay alternately in the (120) and ($1\bar{2}0$) planes, which are equivalent in the crystallographic structure of coesite (Fig. 4b). As the tetrahedral character of the network is gradually lost, more octahedra appear and the planes grow until they interfere with one another. At the top of the enthalpy barrier (Fig. 4c) almost all silicon atoms are sixfold coordinated. The arrangement of the octahedra already shows a preferred layering in the (120) plane, but several defects are present as some chains of edge-sharing octahedra are still aligned in the competing symmetric ($1\bar{2}0$) plane. Finally, the enthalpy undergoes a large drop and a perfect α-PbO_2 structure is created. It consists of an ABAB stacking of (120) planes of edge-sharing octahedra arranged according to a 2×2 pattern[17] (Fig. 4d). In another simulation at higher pressure (335 kbar) and room temperature, we observed that coesite is unstable and rebonding already occurs during the structural optimization. Nevertheless, the same transition to the α-PbO_2 structure is found. Therefore, we make the prediction that by appropriately modifying the experimental protocol, a direct transition from coesite to the α-PbO_2 structure can be observed. We note that the transition from coesite to the α-PbO_2 structure is accompanied by a pronounced volume drop of 24%, which is mainly achieved by shrinkage of the *b* axis (∼15%). Therefore, to observe this phase transition experimentally, we suggest applying a uniaxial compression along the *b* axis to coesite.

In conclusion, here we present several new transformation paths and new predictions for structural transitions in silica polymorphs. Owing to the efficiency of the improved metadynamics algorithm, which allows complex reconstructive transitions with several intermediate states to be simulated, it was possible to bring simulations much closer to thermodynamic conditions and also to much better agreement with experiment.

METHODS

In our classical metadynamics simulations we used the DL POLY MD code (W. Smith, M. Leslie and T. R. Forester, CCLRC, Daresbury Laboratory, Daresbury, England, Version 2.14). We typically used, for each metastep, a 5–12 ps MD run carrying out a constant volume and constant temperature simulation with the Berendsen thermostat, equilibrating for 2.5 ps. In the *ab initio* calculations we adopted the GGA functional developed by Perdew *et al.*[30] and norm-conserving pseudopotentials. In static calculations carried out by the ABINIT package[31], a plane wave basis set with a cutoff of 70 Ry was used. The total energy was integrated on Monkhorst–Pack meshes of *k*-points that guarantee a convergence within 10^{-5} hartree. In the case of anatase, we used a $4 \times 4 \times 2$ Monkhorst–Pack mesh. The *ab initio* metadynamics was carried out using the CPMD code (CPMD V3.9 Copyright IBM Corp 1990–2004, Copyright MPI für Festkörperforschung Stuttgart 1997–2001), the above-mentioned pseudopotentials and a plane wave cutoff of 60 Ry. Each metastep consists of 5,000 MD steps, which amounts to a simulated time of 0.75 ps.

Received 7 March 2006; accepted 6 June 2006; published 16 July 2006.

References

1. Hemley, R. J., Prewitt, C. T. & Kingma, K. J. *Silica—Physical Behaviour, Geochemistry, and Materials Applications 41* (*Rev. Mineral.* Vol. 29, MSA, Washington DC, 1994).
2. Tsuchida, Y. & Yagi, T. New pressure-induced transformations of silica at room temperature. *Nature* **347,** 267–269 (1990).
3. Kingma, K. J., Hemley, R. J., Mao, H. K. & Veblen, D. R. New high-pressure transformation in α-quartz. *Phys. Rev. Lett.* **70,** 3927–3930 (1993).
4. Dubrovinsky, L. S. *et al.* Experimental and theoretical identification of a new high-pressure phase of silica. *Nature* **388,** 362–365 (1997).
5. Haines, J., Léger, J. M., Gorelli, F. & Hanfland, M. Crystalline post-quartz phase in silica at high pressure. *Phys. Rev. Lett.* **87,** 155503 (2001).
6. Kuwayama, Y., Hirose, K., Sata, N. & Ohishi, Y. The pyrite-type high-pressure form of silica. *Science* **309,** 923–925 (2005).
7. Hemley, R. J., Jephcoat, A. P., Mao, H. K., Ming, L. C. & Manghnani, M. H. Pressure-induced amorphization of crystalline silica. *Nature* **334,** 52–54 (1988).
8. Tsuneyuki, S., Matsui, Y., Aoki, H. & Tsukada, M. New pressure-induced structural transformations in silica obtained by computer simulation. *Nature* **339,** 209–211 (1989).
9. Binggeli, N., Chelikowsky, J. R. & Wentzcovitch, R. M. Simulating the amorphization of α-quartz under pressure. *Phys. Rev. B* **49,** 9336–9340 (1994).
10. Somayazulu, M. S., Sharma, S. M. & Sikka, S. K. Structure of a new high pressure phase in α-quartz determined by molecular dynamics studies. *Phys. Rev. Lett.* **73,** 98–101 (1994).
11. Dean, D. W., Wentzcovitch, R. M., Keskar, N., Chelikowsky, J. R. & Binggeli, N. Pressure-induced amorphization in crystalline silica: Soft phonon modes and shear instabilities in coesite. *Phys. Rev. B* **61,** 3303–3309 (2000).
12. Klug, D. D. *et al.* Ab initio molecular dynamics study of the pressure-induced phase transformations in cristobalite. *Phys. Rev. B* **63,** 104106 (2001).
13. Campañá, C., Müser, M. H., Tse, J. S., Herzbach, D. & Schöffel, P. Irreversibility of the pressure-induced phase transition of quartz and the relation between three hypothetical post-quartz phases. *Phys. Rev. B* **70,** 224101 (2004).
14. Martoňák, R., Laio, A. & Parrinello, M. Predicting crystal structures: The Parrinello-Rahman method revisited. *Phys. Rev. Lett.* **90,** 075503 (2003).
15. Laio, A. & Parrinello, M. Escaping free-energy minima. *Proc. Natl Acad. Sci. USA* **99,** 12562–12566 (2002).
16. Demuth, T., Jeanvoine, Y., Hafner, J. & Ángyán, J. G. Polymorphism in silica studied in the local density and generalized-gradient approximations. *J. Phys. Condens. Matter* **11,** 3833–3874 (1999).
17. Teter, D. M., Hemley, R. J., Kresse, G. & Hafner, J. High pressure polymorphism in silica. *Phys. Rev. Lett.* **80,** 2145–2148 (1998).
18. Oganov, A. R., Gillan, M. J. & Price, G. D. Structural stability of silica at high pressures and temperatures. *Phys. Rev. B* **71,** 064104 (2005).
19. Parrinello, M. & Rahman, A. Crystal structure and pair potentials: A molecular-dynamics study. *Phys. Rev. Lett.* **45,** 1196–1199 (1980).
20. Martoňák, R. *et al.* Simulation of structural phase transitions by metadynamics. *Z. Kristallogr.* **220,** 489–498 (2005).
21. Ceriani, C. *et al.* Molecular dynamics simulation of reconstructive phase transitions on an anhydrous zeolite. *Phys. Rev. B* **70,** 113403 (2004).
22. Oganov, A. R., Martoňák, R., Laio, A., Raiteri, P. & Parrinello, M. Anisotropy of Earth's D″ layer and stacking faults in the $MgSiO_3$ post-perovskite phase. *Nature* **438,** 1142–1144 (2005).
23. Raiteri, P., Martoňák, R. & Parrinello, M. Exploring polymorphism: the case of benzene. *Angew. Chem. Int. Edn* **44,** 3769–3773 (2005).
24. van Beest, B. W. H., Kramer, G. J. & van Santen, R. A. Force fields for silicas and aluminophosphates based on ab initio calculations. *Phys. Rev. Lett.* **64,** 1955–1958 (1990).
25. Saika-Voivod, I., Sciortino, F., Grande, T. & Poole, P. H. Phase diagram of silica from computer simulation. *Phys. Rev. E* **70,** 061507 (2004).
26. Choudhury, N. & Chaplot, S. L. Ab initio studies of phonon softening and high-pressure phase transitions of α-quartz SiO_2. *Phys. Rev. B* **73,** 094304 (2006).
27. Sowa, H. & Koch, E. Group-theoretical and geometrical considerations of the phase transition between the high-temperature polymorphs of quartz and tridymite. *Acta Crystallogr.* A **58,** 327–333 (2002).
28. Hantsch, U. *et al.* Theoretical investigation of moganite. *Eur. J. Mineral.* **17,** 21–30 (2005).
29. Car, R. & Parrinello, M. Unified approach for molecular dynamics and density-functional theory. *Phys. Rev. Lett.* **55,** 2471–2474 (1985).
30. Perdew, J. P., Burke, K. & Ernzerhof, M. Generalized gradient approximation made simple. *Phys. Rev. Lett.* **77,** 3865–3868 (1996).
31. Gonze, X. *et al.* First-principles computation of material properties: the ABINIT software project. *Comput. Mater. Sci.* **25,** 478–492 (2002).

Acknowledgements

We would like to acknowledge stimulating discussions with M. Bernasconi as well as help from P. Raiteri and M. Valle.
Correspondence and requests for materials should be addressed to R.M.
Supplementary Information accompanies this paper on www.nature.com/naturematerials.

Competing financial interests

The authors declare that they have no competing financial interests.